Lee et al. Int J Concr Struct Mater (2019) 13:39
https://doi.org/10.1186/s40069-019-0351-2

International Journal of Concrete Structures and Materials

RESEARCH

Open Access

A Study on the Drying Shrinkage and Mechanical Properties of Fiber Reinforced Cement Composites Using Cellulose Nanocrystals

Hyung-Joo Lee, Seung-Ki Kim, Heon-Seok Lee and Woosuk Kim*

Abstract

As part of the research on cement composites using cellulose nanocrystal (CNC) aqueous solution instead of general water, this study produced high-toughness cement composites reinforced with flax and steel fibers to improve the tensile deformation capacity, assessing the isothermal conduction calorimetry analysis, drying shrinkage, and strength characteristics. The mixing amount of CNCs was 0.4, 0.8, and 1.2 vol.% by volume of cement, and an aqueous solution was prepared using the ultrasonication dispersion method. When comparing the results of the experiment according to the CNC mixing ratio, CNCs at 0.8 vol.% led to an improvement in the shrinkage rate and mechanical performance compared with the plain specimen.

Keywords: cellulose nanocrystals, drying shrinkage, strength properties, isothermal conduction calorimetry analysis

1 Introduction

Cellulose nanocrystals (CNCs) are characterized by strong rigidity because they consist only of crystalline regions, with the noncrystalline regions extracted from nanocellulose (Yoon 2016). Cao et al. (2015) reported that CNCs acted as a water pathway in the unhydrated part of a cement core; as a result, hydration was affected, resulting in a 30% improvement in the cement paste compared with plain cement (Cao et al. 2015). Currently, studies on CNC cement have been conducted on cement paste type. In this study, to improve the tensile deformation capacity of cement composites, we intend to propose a new construction material that is more durable and superior in structural performance through the production of high strength cement composites reinforced with fibers.

Therefore, in this study, CNCs were prepared with various concentration ratios (0.4, 0.8, or 1.2 vol.% volume of cement) using the ultrasonication dispersion method, and the drying shrinkage and mechanical properties of high-toughness cement composites reinforced with flax and steel fibers were investigated.

The existing literature on nanocellulose cement and previous studies on strength and shrinkage in relation to this study are summarized in Table 1.

2 Experimental Method

In this study, isothermal conduction calorimetry analysis, strength testing, and drying shrinkage experiments were conducted to quantitatively investigate the reactivity of CNCs in OPC (Ordinary Portland Cement). The hydration heat characteristics of CNCs were analyzed using a micro hydration heat test, and the mechanism of the influence of CNCs on strength was examined based on isothermal conduction calorimetry analysis in strength testing and drying shrinkage experiments.

2.1 Cellulose Nanocrystals (CNCs)

The CNCs used in this experiment were 'C' company products from Canada, and their physical properties are shown in Table 2. The raw CNCs were in powder form,

*Correspondence: kimw@kumoh.ac.kr
Department of Architectural Engineering, Kumoh National Institute of Technology, 61 Daehak-ro, Gumi, Gyeongsangbuk-do 39177, Republic of Korea
Journal information: ISSN 1976-0485 / eISSN 2234-1315

Table 1 Analysis of existing research.

Authors	Synopsis
Cao et al. (2016)	In this paper, the method of dispersing CNC agglomerates using ultrasonic wave was used to improve the cement paste strength up to 50%. These results show that the improvement of the strength of raw CNC (20–30%) in the previous study shows that the dispersion of CNC is a key to improving the flexural strength of cement paste
Mazlan et al. (2016)	In this study, the relationship between the density of cement mortar and the ultrasound velocity (UPV) was studied after the addition of CNC additives as a positive development of compressive strength. The formation of calcium-silicate-hydrate (CSH) gel at a CNC concentration of 0.2% improved, thus improving the strength of up to 42–45% cement composites
Fu et al. (2017)	This work examines the influence of various raw material sources and processing techniques used to make CNCs. In total, nine different CNCs were investigated with pastes made using Type I/II and Type V cements. Isothermal calorimetry (IC), thermogravimetric analysis (TGA), and ball-on-three-ball (B3B) tests were conducted to quantify the performance of the CNC-cement composites. Experimental results showed that the increase in total heat release was greater in Type V than in Type I/II cements, and the intensity increased by 20%
Kim et al. (2006)	The application properties of synthetic fibers for controlling early cracks in concrete were investigated. This study applied polypropylene, cellulose, and nylon fibers. Reduction of crack length and area was observed after fiber incorporation
Kim and Yoon (2016)	The mechanical and self-shrinkage properties of cement Composites were investigated. Tensile and flexural strengths respectively improved by 49.7% and 38.8%. The degree of self-shrinkage decreased to 18.9% after 1 day, and to 5.9% 28 days after nanocellulose incorporation
Peters et al. (2010)	This study was conducted to improve the toughness of reactive powder concrete using nanocellulose and microcellulose fibers. The addition of up to 3% micro- and nanofibers increased the fracture energy by more than 50% relative to the unreinforced material
Jiang et al. (2016)	The early-age self-shrinkage behavior of cement paste containing waste paper fibers under sealed conditions was investigated. The waste paper fiber reduced the self-shrinkage at additions of 0.2% by mass of cement. The waste paper fibers could enhance the self-curing efficiency of cement paste under a low water–cement ratio
Kim et al. (2014)	This paper investigated the behavior of inorganic resin, carbon fiber reinforced polymer (CFRP) composites and resin–concrete interfaces at temperatures ranging from 25 to 200 °C using CFRP. The properties of the inorganic resin showed a strong dependence on the curing time and were influenced by the degree of temperature exposure, and CFRP composites showed a decrease in strength and modulus as temperature increased. In addition, the inorganic resin showed higher thermal stability than the organic resin, but the stress transmission was insufficient and the strength was low

Table 2 Physical properties of CNCs. (Adapted from 'C' company).

Parameter	Product form	Appearance (color)	Crystallite density	Specific surface area	Particle diameter (crystallite)	Particle length (crystallite)	pH
Specification	Powder	White	1.5 g/cm^3	400 m^2/g	2.3–4.5 nm (by AFM)	44–108 nm (by AFM)	6–7

as shown in Fig. 1, and SEM (Scanning Electron Microscope) analysis determined they had a spherical shape and TEM (Transmission electron Microscope) analysis showed a rod shape for dispersed CNCs.

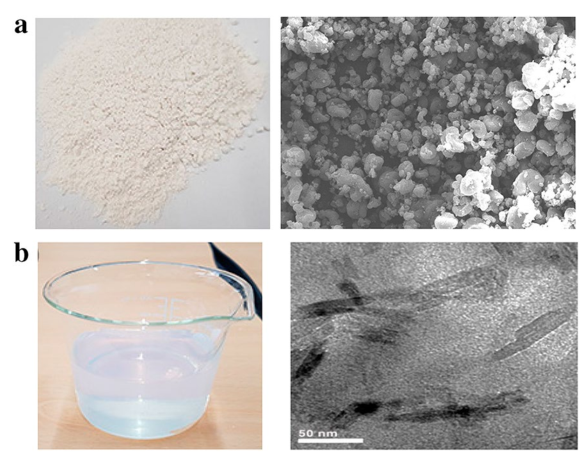

Fig. 1 CNCs before and after dispersion: **a** powder type CNCs and SEM analysis (up). **b** Aqueous solution type CNCs and TEM analysis (down).

2.2 Isothermal Conduction Calorimetry Analysis

Cao et al. (2015) reported that, while cement is curing, the hydration product forms a shell around the hydrated cement particles to slow water diffusion into the membrane, i.e., into the cement core (Cao et al. 2015).

CNCs enhance the hydration of unhydrated cement cores and affect the hydration product C-S-H (calcium silicate hydrate), resulting in increased strength (Cao et al. 2016). In this experiment, isothermal conduction calorimetry was analyzed for 7 days for plain cement using general water and cement using aqueous solutions of CNCs with mixing ratios of 0.4, 0.8, or 1.2 vol.%. Table 3 shows the variables for the isothermal conduction calorimetry analysis.

Table 3 Isothermal conduction calorimetry analysis variables.

Classification	Plain	C04	C08	C12
Contents	Cement + water	Cement + CNCs suspension (CNCs: vol.% compared with cement)		

Fig. 2 Gel type CNCs.

2.3 CNC Dispersion Method

The nanoparticles have a relatively large Van der Waals attractive force, which has a greater impact than other effects, resulting in a large aggregation of particles. To eliminate this aggregation, mechanical dispersion and nanoparticle surface treatment can be used to reduce van der Waals attraction or to prevent electrostatic repulsion or steric hindrance (Kim et al. 2016). Generally, mechanical dispersion methods include ultrasonic dispersion and high pressure dispersion. In this experiment, CNCs were dispersed using ultrasonic dispersion. High-pressure dispersion is considered to be an appropriate dispersion method because the variation in the particle size distribution is small and the average diameter according to the pressure is less than the ultrasonic dispersion (Lee et al. 2019). However, high-pressure dispersion requires a specialist company that has expensive dispersing equipments to produce samples, and it is not provided sufficient to carry out the experiment. Therefore, the experiment was conducted using ultrasonic dispersion which can be used as nanomaterial and can be dispersed at the laboratory level. On the surface of CNCs, numerous hydroxyl groups exist (Mehta and Monteiro 2013), and when the CNCs were added to water, they were observed to form a gel, as shown in Fig. 2, through hydrogen bonding. In this case, as the amount of energy required for dispersion increased, and the dispersion process was carried out for a long period of time, it was determined that physical properties caused by sample damage would not be exhibited. As the solvent agent, primary purification distilled water was used.

Fig. 3 Drying shrinkage test set-up.

2.4 Drying Shrinkage Measurement

A rectangular mold ($40 \times 40 \times 160$ mm) with a hole at both ends was used, as shown in Fig. 3, to analyze the drying shrinkage characteristics of the cementitious composites. As shown in Fig. 4, the embedded gauge was placed at the center of the specimen so that it would not be disturbed by shrinkage. The gauge was fixed with wires, and a 1-mm-thick Teflon® sheet was placed on the bottom and both ends of the mold to prevent the movement of the specimen from being restrained by the mold (Yoo et al. 2010).

The cementitious composites were then formed according to the various parameters and covered with polyester film to prevent water evaporation and absorption. The autogenous shrinkage strain was measured for 24 h after cementitious composite formation, and the specimens were then demolded. Drying shrinkage strain was measured for 60 days under constant temperature and humidity conditions by sealing all the exposed surfaces with aluminum tape to prevent specimen drying. Table 4 lists the mixing ratios of the test specimens. The reason for the difference in the amount of superplasticizer is due to the hydration promoting characteristic of CNC, and as the amount of CNC increases, the initial setting time due to the temperature rise due to the influence of initial hydration is faster than that of plain specimen. Therefore, as the amount of CNC increases, hydration reaction amount also increases, so the amount of superplasticizer is increased to secure the fluidity.

The fiber used in the experiment was flax fiber (cellulose type natural fiber) and steel fiber (generally used for fiber reinforcement), and its physical properties are shown in Table 5.

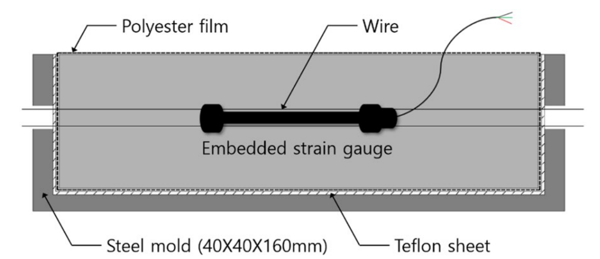

Fig. 4 Embedded strain gauge detail.

2.5 Evaluation of Strength Characteristics

The compressive and flexural strengths were evaluated to determine the mechanical properties of cement composites with CNCs and fiber reinforcement. The test specimens were prepared with dimensions of $50 \times 50 \times 50$ mm for compressive strength and tested in accordance with KS L 5105. For the flexural strength, $40 \times 40 \times 160$ mm specimens were prepared and tested according to KS F 2408. The mixing proportions were the same as those used in the drying shrinkage experiment.

3 Experimental Results

3.1 Isothermal Conduction Calorimetry Analysis

Since cement hydration is an exothermic reaction, heat flow and cumulative calorific value are directly related to hydration rate and hydration degree (DOH). Therefore, micro hydration analysis was performed to analyze the hydration characteristics of cement with CNC incorporation. Figure 5 shows the results of isothermal conduction calorimetry analysis conducted for 7 days on cement with various amounts of CNCs. The first heat flow peak occurred within 1 h for all variables. However, the first heat flow peak value of cement with CNCs was 50% or more of that for plain cement (without CNCs). These results suggest that the heat of dissolution of aluminate

Table 4 Mixing proportion design.

Classification	Water	Cement	Fly ash (cement replacement %)	Super plasticizer (wt%)	Fiber (vol.%)	CNCs (vol.% compared with cement)
Plain	1	3	–	0.25	1 (use for strength evaluation)	–
C04			25	0.75	–	0.4
C04F1					1	
C04S1						
C08				1.25	–	0.8
C08F1					1	
C08S1						
C12				2.25	–	1.2
C12F1					1	
C12S1						

F flax fiber, *S* steel fiber, *1* fiber vol.%.

Table 5 Fiber physical properties.

Classification	Density	Length (mm)	Diameter (µm)	Tensile strength (MPa)	Young's modulus (GPa)
Flax fiber 	1.5	10	40–600	345–1500	27.6
Steel fiber 	7.75	13	200–600	400–20,000	200

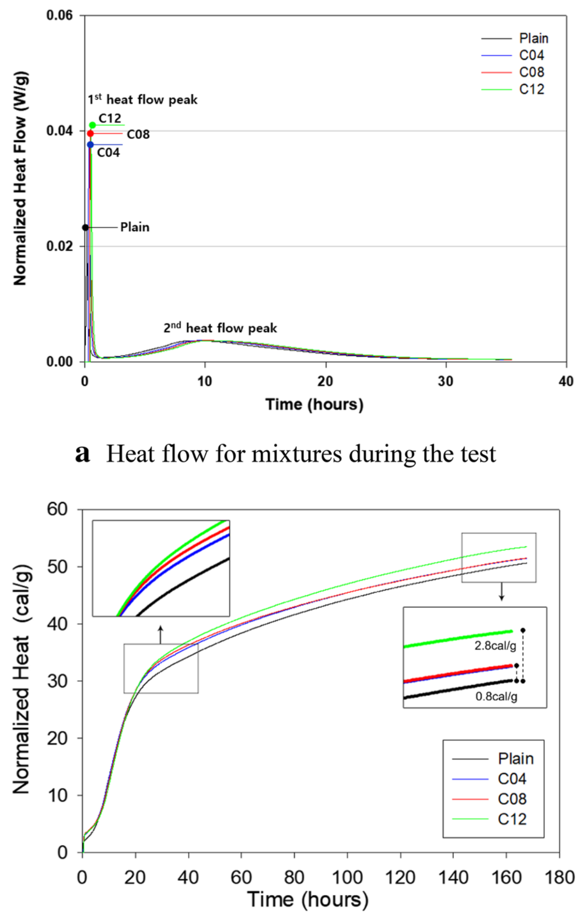

a Heat flow for mixtures during the test

b Cumulative heat for mixtures during the test

Fig. 5 Isothermal conduction calorimetry analysis results.

and sulfate solution is higher than that of OPC because of the incorporation of CNCs (Lin et al. 2012). In the case of plain cement without CNCs, the secondary heat flow peak appeared at approximately 9 h; this peak also appeared at approximately 9 h for C04, and at approximately 10 h for C08 and C12. In addition, the cumulative heat released increased in the specimens containing CNCs compared with plain cement.

3.2 Drying Shrinkage

After cementitious composite formation, the composites expanded for approximately 24 h; after that, the shrinkage strain increased sharply up to approximately 30 days, and thereafter, it tended to gently increase. In the case of the plain specimen, the shrinkage showed a rapid increase up to early on the 7th day. However, when the CNCs were mixed, the shrinkage strain tended to increase relatively gently over the first 30 days.

Figure 6a shows the result of analysis of drying shrinkage strain according to the volume fraction of CNCs. The final drying shrinkage strain of the plain specimen at 60 days was − 874.95 μm, and when CNCs were mixed, the drying shrinkage strain of C04 was − 666.43 μm, that of C08 was − 394.14 μm, and that of C12 was − 765.10 μm. Eventually, the drying shrinkage-reducing performance was improved by mixing CNCs. In particular, when 0.8% volume fraction of CNCs was added, the shrinkage-reducing performance was the best, showing a 55% reduction compared with the plain specimen.

Figure 6b, c show the results of analysis of shrinkage strain according to the type of fiber. The shrinkage strains of specimens mixing both CNCs and fibers did not differ significantly with the volume fraction of CNCs. However, the shrinkage-reducing performance of specimen series incorporating a 0.8% volume fraction of CNCs was the best. The final shrinkage strain of C08F1, with flax fibers, was − 460.57 μm, and that of C08S1, with steel fibers, was − 612.05 μm; the shrinkage strains were reduced by 47.4% and 30%, respectively, compared with the plain specimen. Eventually, the shrinkage-reducing performance of the specimen with flax fibers was superior to that with steel fibers.

Figure 6d reveals that, overall, the shrinkage-reducing performance of the specimens mixing both CNCs and flax fibers was the best, except for that of the C08 specimen.

The experimental results confirmed that the shrinkage-reducing performance is improved by incorporating CNCs. These results suggest that the evaporation amount of surplus water involved in hydration reaction is less than Plain due to the effect of hydration reaction promoting properties of CNCs. It can be confirmed that this experimental result is consistent with the results described in previous studies (Ardanuy et al. 2015) about the relationship between the hydration reaction and the strength development because the strength of the C08 specimen, with the highest shrinkage-reducing performance, is the highest. Also, as shown in the results of hydration heat measurement, in the case of Plain and C04 and C08, there is no difference in accumulated heat, but cumulative calorific value at C12 is more than three times higher than C04 and C08. As the CNC content increases, the hydration reaction is promoted and the amount of ettringite increases. As a result, the shrinkage rate is reduced because the expansibility is increased. However, the shrinkage ratio of C12 was rather increased. It is considered that the shrinkage reduction performance due to the incorporation of CNC is somewhat reduced because the dispersion of CNC in the cement is not properly performed due to the incorporation of a large amount of CNC (Table 6).

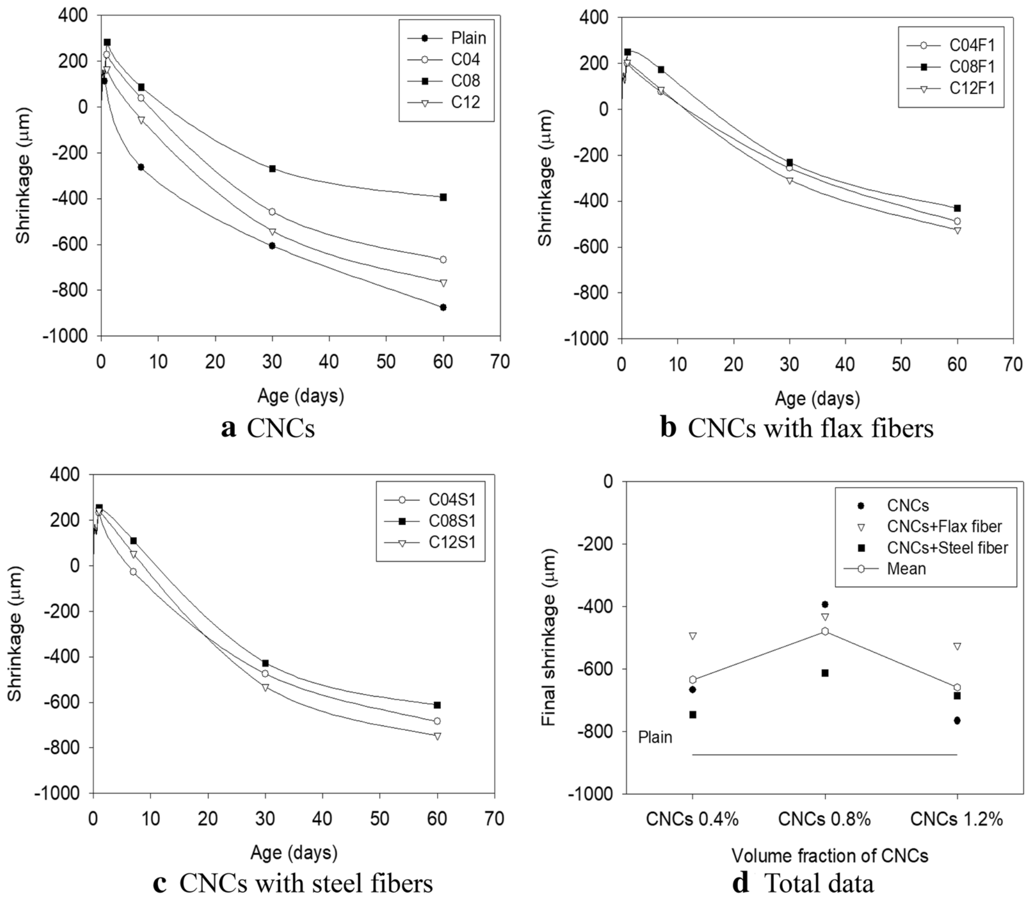

Fig. 6 Drying shrinkage curves.

Table 6 Drying shrinkage strain of cementitious composites over time.

Series	Final shrinkage (μm)			
	1 day	7 days	30 days	60 days
Plain	111.43	− 264.08	− 606.67	− 874.95
C04	227.62	37.62	− 459.05	− 666.43
C04F1	200.95	75.95	− 256.71	− 490.10
C04S1	242.86	52.86	− 475.29	− 684.72
C08	282.86	86.86	− 268.81	− 394.14
C08F1	249.52	173.52	− 232.19	− 430.57
C08S1	254.29	110.29	− 427.57	− 612.05
C12	165.71	− 54.29	− 542.00	− 765.10
C12F1	205.71	85.71	− 308.00	− 524.76
C12S1	233.33	− 26.67	− 531.81	− 746.00

3.3 Strength

The results of compression testing are shown in Fig. 7 according to fiber type to evaluate the effect of fiber addition. In the specimens without CNCs, the flax fiber was not an effective compressive strength reinforcement for cement composites; rather, it reduced the compressive strength compared with the plain specimen, similar to results reported in a previous study (Kang et al. 2010). However, the steel fibers improved the compressive strength. These results were judged to be related to the fiber stiffness and density. When fibers are mixed in cement composites, the fibers replace parts of the cement composites, which means that the total density and stiffness decrease. However, steel fibers have higher density and stiffness than flax fibers, which leads to the increase

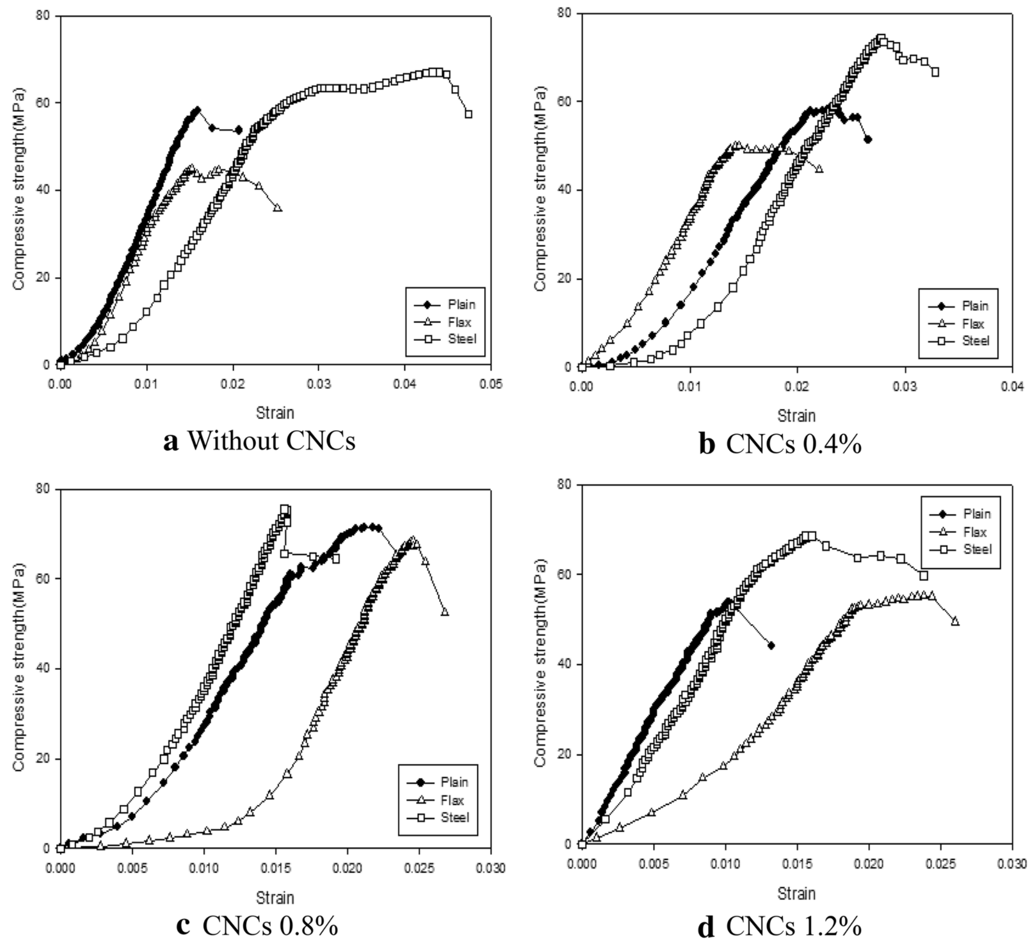

Fig. 7 Stress–strain curves of compression tests according to fiber type.

in compressive strength compared with flax fiber specimens (Gwon et al. 2015).

The compressive strength properties according to CNC ratio are shown in Fig. 8 to evaluate the effect of CNC addition. The 0.8% CNC specimens showed outstanding performance. In the specimens without fibers, the 0.8% CNC specimen showed a strength improvement from 10 to 20% compared with other specimens. In the specimens with flax fibers, a similar trend was observed as in specimens without fibers. The addition of CNCs in specimens with steel fibers was not effective compared with the specimens without fibers or with flax fibers. The results suggest that 0.8% CNCs is the optimal ratio.

The comprehensive data for compression tests are shown in Fig. 9. We verified that 0.8% CNCs is the optimal ratio once more through this graph. Comparing the strength improvement ratio with or without CNCs, 0.4%, 0.8%, and 1.2% CNCs showed respective improvements of 0%, 23%, and − 8% in the specimens without fibers, 11%, 53%, and 23% in the specimens with flax fibers, and 10%, 12%, and 2% in the specimens with steel fibers. The addition of 0.4% and 1.2% CNCs led to a slight improvement in performance. However, the strength was reduced in specimens without fibers. The effect of CNCs was most pronounced in the specimens incorporating 0.8% CNCs, both without fibers and with flax fibers.

Flexural test results are as shown in Fig. 10 according to fiber type which is to evaluate the effect of fiber. The flax fiber was not an effective reinforcement material for cement composites. Rather, the flexural strength decreased compared with that of the plain specimen when flax fibers were mixed with 0.4% and 0.8% CNCs. This result means that flax fiber is not suitable to reinforce the strength of cement composites. The specimens with steel fibers indicated superior strength, regardless of the CNC ratio. The composites with steel fibers were more ductile than other specimens, except for the plain specimen (Mun et al. 2015).

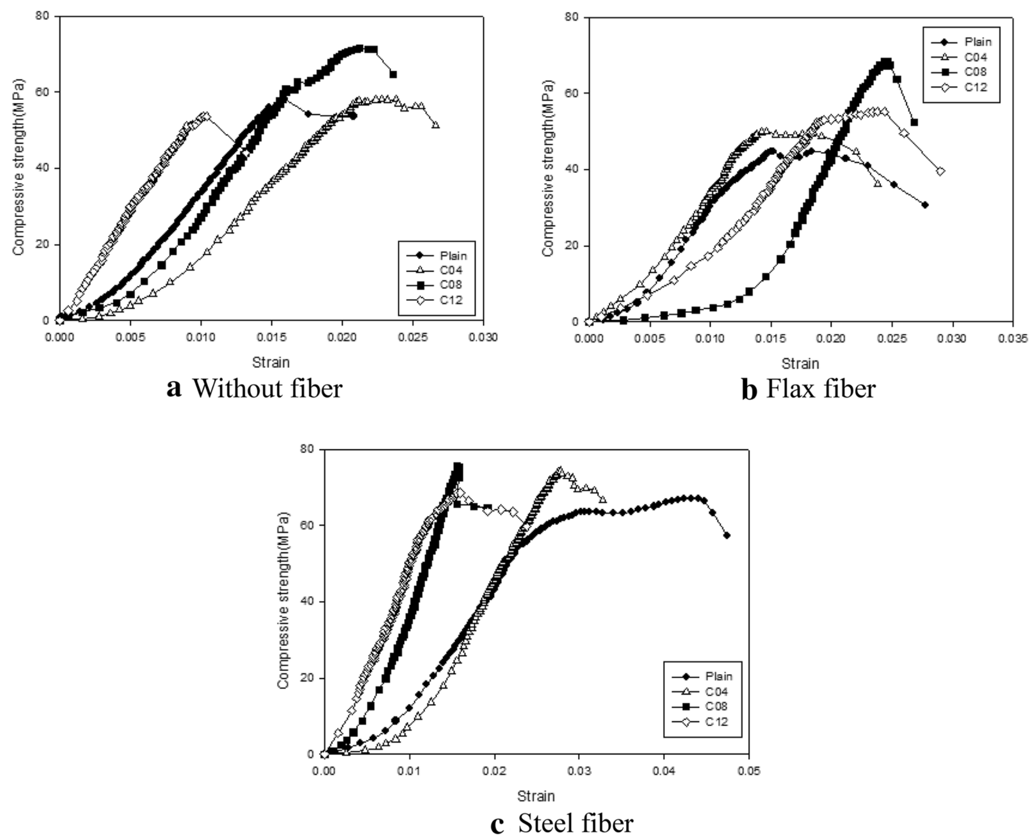

Fig. 8 Stress–strain curves of compression tests according to CNC ratio.

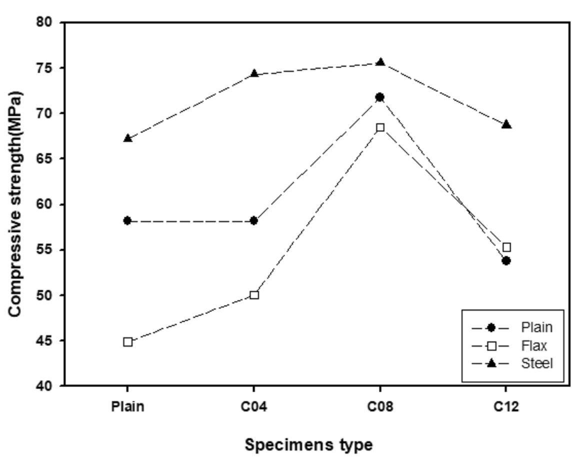

Fig. 9 Compressive strength trend of compression tests.

The flexural results are shown in Fig. 11 according to CNC ratio. The 0.8% CNC specimens had the highest strength without reference to fiber type, with the strength decreasing in the order of 0.4% CNCs and 1.2% CNCs. The strength change according to CNC ratio was observed in the plain specimens. However, the specimens with flax fibers only indicated a slight strength change according to CNC ratio.

The comprehensive data of the flexural tests are shown in Fig. 12. The results suggest that 0.8% CNCs and steel fibers are most effective reinforcement for cement composites. The strength improvements of 0.4% CNCs and 0.8% CNCs were respectively 40% and 58% compared with the plain specimen without CNCs and without fibers. The specimen with 0.8% CNCs and steel fibers indicated a 70% strength increase compared with the plain specimen with steel fibers and a 200% increase compared with the plain specimen without fibers. The specimens using flax fibers had almost the same values, regardless of the CNC ratio.

We can therefore conclude that the optimal ratio of CNCs is a 0.8% volume fraction of cement through mechanical testing of cement composites using aqueous solutions of CNCs.

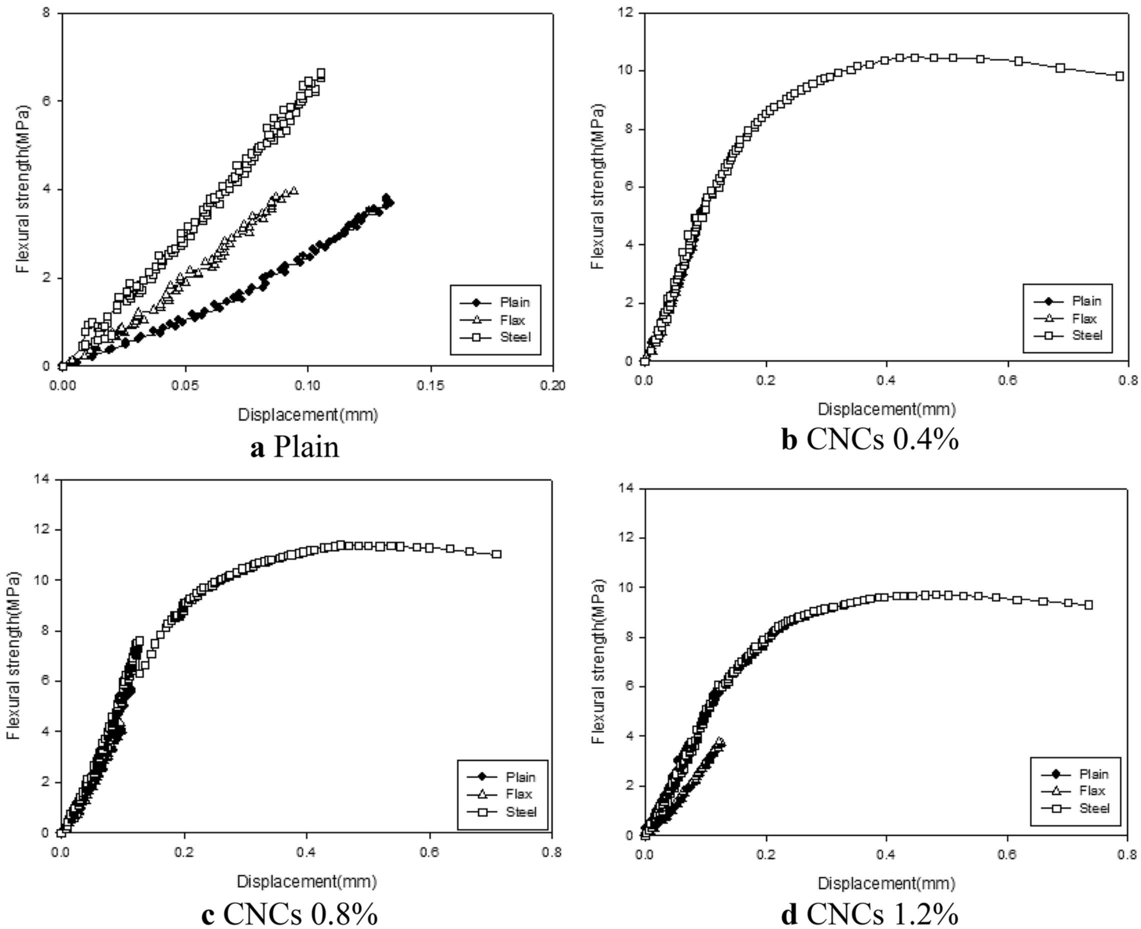

Fig. 10 Stress–displacement curves of flexural tests according to fiber type.

4 Conclusions

This study was carried out to quantitatively determine the performance of fiber-reinforced cement composites according to the mixing ratio of CNCs. The conclusions are as follows.

1. As a result of isothermal conduction calorimetry analysis, the maximum primary calorific value of the specimens containing CNCs increased by up to 50% compared with the plain cement specimen. This is attributed to the increase in the calorific value of the aluminate and sulfate solutions caused by the effect of the CNCs on the hydration reaction in the cement.
2. The CNCs can effectively reinforce the compressive and flexural strength of cement composites. The trend of strength improvement was observed for all specimens containing CNCs. The outstanding strength improvement was shown with the addition of 0.8% CNCs by volume of cement. The fiber type also affected the improvement ratio. This ratio was reduced after the addition of flax fibers. However, the specimens containing steel fibers showed an increased improvement ratio compared with the plain cement specimens. We have determined that this result occurred because the water absorption by the flax fibers competed with the enhancement of the hydration of cement by CNCs. However, it is possible to have this kind of strength improvement in specimens containing steel fibers because the steel fibers only slightly affected the properties of CNCs compared with the flax fibers.
3. Drying shrinkage tests revealed that the shrinkage decreased in all specimens when CNCs were used. There was a 55% reduction compared with that of the plain concrete specimen when CNCs were mixed at 0.8% volume fraction, and it was confirmed that the drying shrinkage strain reducing performance was the best. The shrinkage strain associated with the incorporation of flax fibers was 29.7% lower than that with steel fibers, based on the specimen series con-

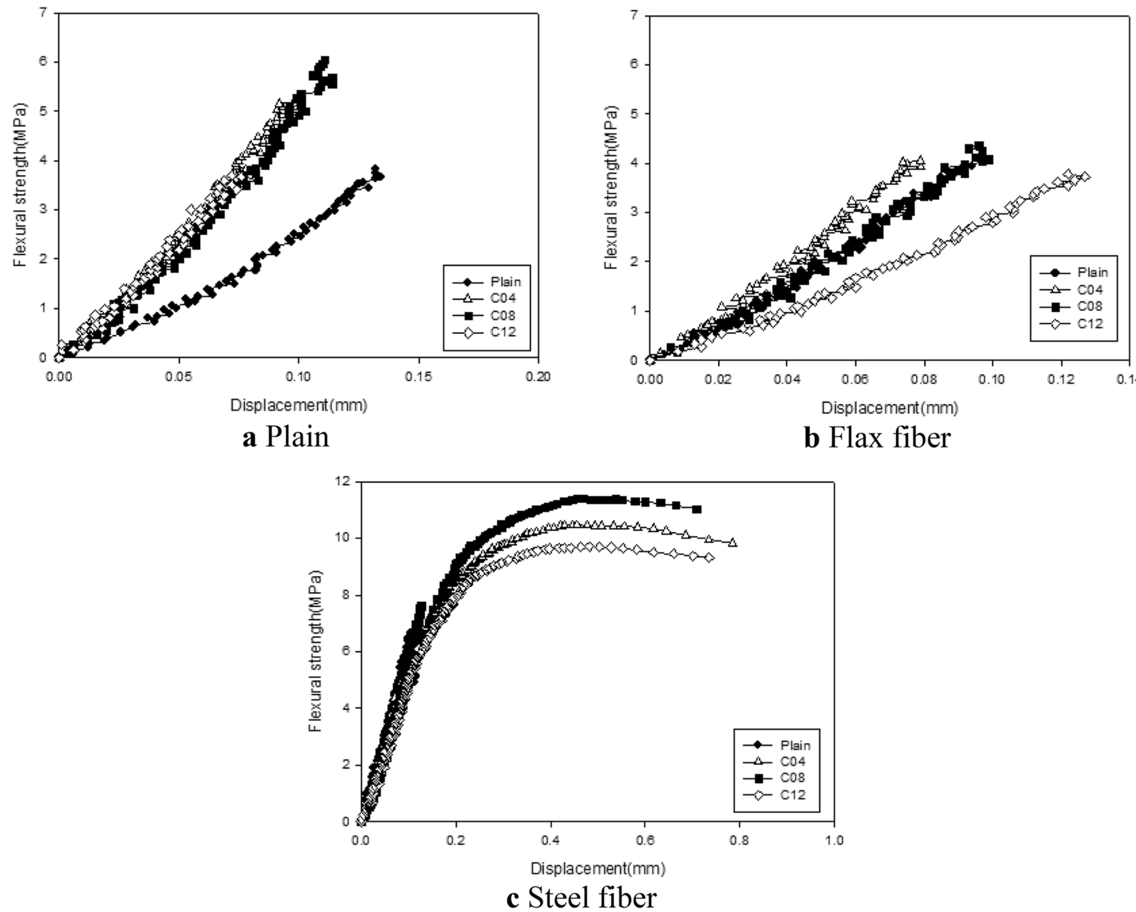

Fig. 11 Stress–displacement curves of flexural tests according to CNC ratio.

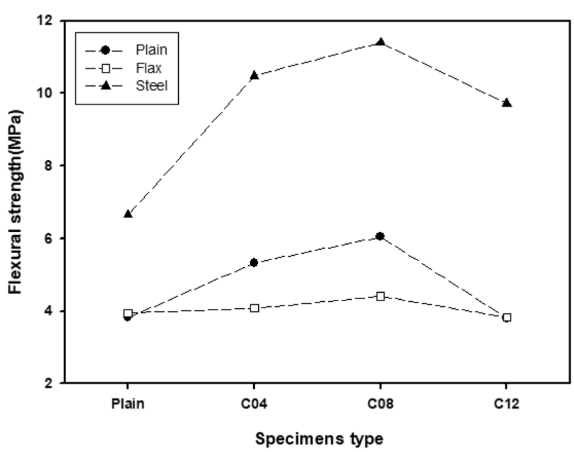

Fig. 12 Flexural strength trend of flexural tests.

taining a 0.8% volume fraction of CNCs. Applying CNCs to various construction materials may effectively improve the shrinkage resistance.

4. In this study, the optimum mixing ratio according to CNCs variables is considered to be CNCs 0.8 vol.%, Which shows the highest shrinkage reduction and strength values. If mass dispersion is possible, CNCs application will be diversified in high strength concrete production.

Acknowledgements

The authors thank the Infrastructure and Transportation Technology Promotion Research Program funded by the Ministry of Land, Infrastructure and Transport of the Korean government, for all funding of this work under the grant [code# 18CTAP-C133534-02].

Authors' contributions

HJL, SKK, and HSL conceived, designed and performed the experiments. WK supervised this project as a principal investigator. WK and HJL analyzed the data and wrote the paper. All authors read and approved the final manuscript.

Availability of data and materials

Not applicable.

Competing interests

The authors declare that they have no competing interests.

Received: 27 February 2019 Accepted: 6 June 2019
Published online: 15 July 2019

References

Ardanuy, M., Claramunt, J., & Toledo Filho, R. D. (2015). Cellulosic fiber reinforced cement-based composites: A review of recent research. *Construction and Building Materials, 79,* 115–128.

Cao, Y., Zavaterri, P., Youngblood, J., Moon, R., & Weiss, J. (2015). The influence of cellulose nano crystal additions on the performance of cement paste. *Cement & Concrete Composites, 56,* 73–83.

Cao, Y., Zavaterri, P., Youngblood, J., Moon, R., & Weiss, J. (2016). The relationship between cellulose nanocrystal dispersion and strength. *Construction and Building Materials, 119,* 71–79.

Fu, T., Montes, F., Suraneni, P., Youngblood, J., & Weiss, J. (2017). The influence of cellulose nanocrystals on the hydration and flexural strength of Portland cement pastes. *Polymers, 9,* 424.

Gwon, S. W., Kim, S. P., Ahn, E. J., & Shin, M. S. (2015). Stress-deformation responses of steel fiber-reinforced cementitious composites in direct tension and flexure. *Proceeding of the Korea Concrete Institute, 2015*(5), 433–434. **(in Korean)**.

Jiang, Z., Guo, X., Li, W., & Chen, Q. (2016). Self-shrinkage behaviors of waste paper fiber reinforced cement paste considering its self-curing effect at early-ages. *International Journal of Polymer Science, 2016,* 8690967.

Kang, S. T., Park, J. J., Ryu, G. S., & Kim, S. W. (2010). The effect of steel-fiber reinforcement on the compressive strength of ultra high performance cementitious composites (UHPCC). *Magazine of the Korea Institute for Structural Maintenance and Inspection, 14*(5), 110–118. **(in Korean)**.

Kim, K., Kim, H., Jung, W., Choi, H., Hong, S., & Hwang, D. (2016). *Nano material*. Changwon: Bumhan Ltd. **(in Korean)**.

Kim, B. G., Kim, K. R., Kwon, Y. J., & Han, C. G. (2006). Synthetic fiber to control the early crack in concrete and application in construction field. *Magazine of the Korea Concrete Institute, 18*(1), 36–43. **(in Korean)**.

Kim, Y., Siriwardanage, T., Hmidan, A., & Seo, J. (2014). Material characteristics and residual bond properties of organic and inorganic resins for CFRP composites in thermal exposure. *Construction and Building Materials, 50*(15), 631–641.

Kim, S. W., & Yoon, B. T. (2016). Effect of nanocellulose on the mechanical and self-shrinkage properties of cement composites. *Applied Chemistry for Engineering, 27*(4), 380–385.

Lee, H., Lee, H., Kang, Y., Seo, J., Kim, W., & Kang, T. (2019). State-of-the-art of cellulose nanocrystals and optimal method for their dispersion for construction-related applications. *Applied Science, 9,* 426–439.

Lin, N., Huang, J., & Dufresne, A. (2012). Preparation, properties and applications of polysaccharide nanocrystals in advanced functional nanomaterials: A review. *Nanoscale, 4,* 3274.

Mazlan, D., Din, M., Tokoro, C., & Ibrahim, I. S. (2016). Cellulose nanocrystals addition effects on cement mortar matrix properties. *International Journal of Advances in Mechanical and Civil Engineering, 3,* 44–48.

Mehta, K., & Monteiro, P. (2013). *Concrete: microstructure, properties and materials*. New York: McGraw-Hill Education.

Mun, Y. B., Kim, H. C., Choi, H. K., Kim, J. Y., Lee, H. S., & Kim, M. K. (2015). An experimental study on hydration and strength development of high blain cement at low temperature. *Journal of the Korea Institute of Building Construction, 15*(4), 367–373. **(in Korean)**.

Peters, S. J., Rushing, T. S., Landis, E. N., & Cummins, T. K. (2010). Nanocellulose and microcellulose fibers for concrete. *Journal of the Transportation Research Board, 2142,* 25–28.

Yoo, D., Min, K., Yang, J., & Yoon, Y. (2010). Evaluation of shrinkage cracking characteristics and degree of restraint for ultra-high-strength concrete. *Journal of the Korea Concrete Institute, 22,* 641–650.

Yoon, H. (2016). A study on the physical/chemical properties of cellulose nanocrystals and its application. *NICE, 34,* 500–504.

Publisher's Note